JOURNAL OF SOLID STATE CHEMISTRY 77, 90–95 (1988)

Rietveld Refinement of the Structure of $Sr_{0.3}Ba_{0.7}FCl$

WIESLAW LASOCHA* AND HARRY A. EICK†

Department of Chemistry, Michigan State University, East Lansing, Michigan 48824

Received April 13, 1987; in revised form June 21, 1988

The structure of $Sr_{0.3}Ba_{0.7}FCl$, formula weight 176.87, was determined by the Rietveld refinement procedure from X-ray powder diffraction data. This structure was solved in space group $P2/n$, $Z = 2$ with $a = 4.335(1)$, $b = 4.304(1)$, $c = 7.146(3)$ Å, and $\gamma = 90.379(2)°$; $R_f = 0.055$, $R_{wp} = 0.141$. The compound exhibits a distorted tetragonal PbFCl-type structure. Interatomic distances are presented and compared with those of SrFCl and BaFCl.

Introduction

Two PbFCl-type solid solution regions and one single-phase region were observed in the $Sr_xBa_{(1-x)}FCl$ system (*1*). One solid solution region spanned $0.0 < x \leq 0.1$; the other $0.6 \leq x < 1.0$. Between these regions, $0.1 < x < 0.6$, a phase which could be indexed on the basis of monoclinic symmetry was observed. The monoclinic angle varied with composition with the greatest deviation from orthogonality occurring at $x \sim 0.3$, i.e., at $Sr_{0.3}Ba_{0.7}FCl$. It was thought that the angular variation might be the result of the cations ordering to achieve better packing. Consequently, the work reported herein was undertaken to determine the structure of this apparently monoclinic phase.

Initial attempts were directed toward growing a single crystal suitable for structural analysis by cooling slowly a fused mixture of the reactants. However, when only microcrystals could be obtained, a structural solution and refinement by the Rietveld procedure was undertaken (*2*).

Experimental

A sample was prepared according to Eq. (1) by following the procedure of Hodorwicz *et al.* (*1*). Interplanar *d*-spacings were determined initially from pulverized portions of the product mixed with NBS calibrated Si [$a_0 = 5.43082(3)$ Å] in a 114.6-mm Guinier X-ray camera with Cu$K\alpha_1$ radiation, $\lambda\alpha_1 = 1.54051$ Å.

$$0.3SrCl_2 + 0.2BaCl_2 + 0.5BaF_2 = Sr_{0.3}Ba_{0.7}FCl \quad (1)$$

Intensity data were collected with a Philips APD3720 PDP MICRO 11 controlled powder diffractometer system with graphite monochromatized Cu$K\alpha$ radiation, sample spinner, and theta-compensating slit. Details of the data collection and refinement procedure are presented in Table I. The Cu$K\alpha_2$ radiation component was stripped with the APD software (*3*). Subsequent cal-

* On leave from Department of Chemistry, Jagiellonian University, Krakow, Poland.

† To whom correspondence should be addressed.

0022-4596/88 $3.00

culations were effected on a VAX 11/750 computer with the program XRS82 (*4*). Polynomial scattering factors and dispersion corrections were used (*5*, *6*). A portion of the sample was examined on a JEOL 120CX electron microscope. The pulverized specimen was suspended in acetone by sonication and picked up on a holey carbon grid by dipping the grid into the solution.

Theta-Compensating Slit Correction

Data were recorded with an automatic divergence slit (ADS). With an ADS the relative intensities of diffracted peaks differ considerably from those measured with a fixed-slit system. To calculate structure factors or to compare the intensity data with that measured with a fixed-slit system, a correction factor must be applied.

In the standard symmetrical reflection technique intensity, I, diffracted at a specific 2θ angle, is given by

$$I = I_0 A/\mu_i, \qquad (2)$$

where μ_i is the linear absorption coefficient and A is the cross-sectional area of the incident beam, I_0, at its point of intersection with the specimen (*7*). In measurements with fixed slits, A is a constant. With an ADS, A changes continuously with θ so that at any angle the same area of the specimen surface is irradiated. Thus on the assumption that the intensity varies linearly with the divergence of the X-ray beam, ADS intensity data must be multiplied by a factor proportional to $1/\sin\theta$. The manufacturer suggests this factor should be $1/\sin\{(11.16° + (79/90)\theta) - 0.19355\}$. Over the range of interest in this work an error of less than 3% results if only $1/\sin\theta$ is used, as was done. Failure to apply this ($1/\sin\theta$) correction leads unavoidably to negative values of either the overall temperature factor or the individual temperature factors because the errors exhibit an angular dependency.

Preferred Orientation

Because the crystallites form small plates perpendicular to [001] preferred orientation effects were of particular concern. In an effort to minimize these effects, a series of specimen planchets was prepared by different procedures. The intensities of the reflections most sensitive to preferred orientation [i.e., (001) and (002)] were examined and the preparation which minimized preferred-orientation effects, well-ground crystals scattered on a glass backing coated with double-sided Scotch tape, was used. Even with this preparation it was noted that the (001) and (002) reflections were relatively more intense in the diffractograms than they were in the Guinier photographs. It was thus necessary to consider this effect in the calculations.

For plate-like crystals the preferred-orientation correction formula is

$$P = \exp[p\cos(2\sigma)]. \qquad (3)$$

In Eq. (3), P, the correction factor, may be expressed in terms of the preferred-orientation factor and σ is the angle between the preferred orientation and the scattering vector for any given reflection. By using I_{obs} values with calculated 2σ angles and intensity values derived in the early stages of refinement, the $\ln(I_o/I_c)$ vs $\cos(2\sigma)$ dependency (Fig. 1) could be approximated and

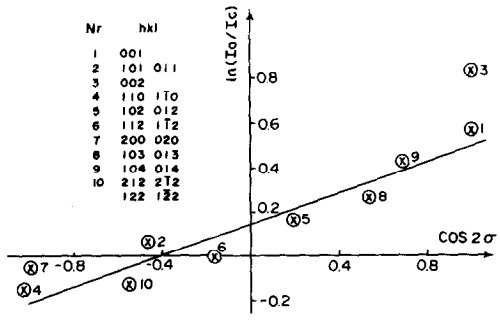

FIG. 1. Plot of the $\ln(I_o/I_c)$ vs $\cos(2\theta)$ dependence which illustrates preferred orientation effects.

from this a preferred-orientation factor starting value, 0.381, obtained. For this plot overlapping reflections were treated as the sum of the calculated and observed intensities of the contributing reflections since they could not be separated very well at this stage of refinement.

Structural Solution

From lattice parameter data for $Sr_xBa_{(1-x)}FCl$, $x = 0.3$, 0.6, and 1.0 (*1*, *8*), it was determined that the monoclinic structure results from a small distortion of the PbFCl (*P4/nmm*) structure. This distortion destroys the fourfold axis and parallel mirror planes. Consideration of the systematic extinction (Table I) limits the structure to monoclinic space groups *P2/n* or *Pn* [in standard setting, *P2/b* or *Pb* with $\gamma = 134.6°$] or to a triclinic space group. We chose the centrosymmetric *P2/n* space group and, for the atomic coordinates not fixed by symmetry, used the average of the SrFCl and BaFCl atomic (*8*) parameters as a starting model for refinement.

A nonoverlapped reflection (002) was selected and a peak-profile function calculated (*4*). This function is calculated from the experimental data and, consequently, any peak shape can be described reasonably accurately. The function refined to an *R* value of 0.076.

After ADS and LP corrections had been applied, refinement began with the scale factor, followed by the scale factor and lattice parameters. After these had stabilized the zero correction, the halfwidth and the asymmetry parameters were refined separately (three cycles for each group of parameters). Finally, all profile parameters and the scale factor were refined together. In subsequent steps atomic parameters were refined first independently and then with isotropic thermal parameters. Reflections collected beyond 65° (2θ) were broad and weak. When corrected by ADS and LP, they contributed little to the refinement; consequently, data beyond 64° (2θ) were eliminated.

When the parameters were all refined together it was noticed that the calculated intensities of strong overlapping reflections (i.e., *hkl*, $h\bar{k}l$ and *hkl*, *khl*) were affected by the zero correction (ZC) parameters. Changes in ZC shift the whole pattern slightly and, as a consequence, affect the relative intensities of the individual reflections. Only the F atom positional and thermal parameters were affected by these shifts. Two procedures were used to minimize this ZC effect and to improve the refinement process. In the first procedure the ZC parameter was determined from the (Guinier camera derived) lattice parameters and the observed pattern and was excluded from the final refinement. In the second procedure the data were supplemented with "soft restrictions" on the Ba–F bond length. These restrictions were assigned weights as defined in the XRS82 system (*4*). Both of these approaches stabilized the F atom position and yielded similar positional and thermal parameters. The data presented in the tables are derived by the first procedure since it was deemed to be of a more general nature. Final values of refined profile and atomic parameters are presented in Tables I and II, respectively.

Results and Discussion

The Guinier data indicated that the preparations were monophasic with lattice parameters close to those reported earlier (*1*). The angle, 90.38°, derived from the Rietveld refinement is almost 1° less than the value reported for this composition, 91.43(7)° (*1*). It was noted that the angle varied with composition and the larger value represented the maximum deviation observed in the phase study. The 90.38° value therefore indicates either that the mixed composition is slightly off stoichiometry, probably as a result of preferential

TABLE I

CRYSTALLOGRAPHIC DATA

Pattern 2θ range (deg)	10–64
Step scan increment (2θ deg)	0.02
Count time (sec/step)	18
Standard peak: *hkl* (2θ)	(002), 24.889°
Space group	$P112/n$
a (Å)	4.335(1)
b (Å)	4.304(1)
c (Å)	7.149(3)
γ (deg)	90.379(2)
Systematic extinction	$hk0$, $h + k = 2n + 1$
Volume (Å^3)	133.17
Density (cal) (g cm^{-3})	2.204
Number of observations	1751
Number of reflections	45
Number of structural parameters	8
Number of profile parameters	10
$R_{expected} = \sqrt{\{N_{obs}/\Sigma(I_i\sigma_i)^2\}}$	0.090
$R_f = \Sigma\lvert F_o - F_c\rvert/\Sigma F_o$	0.055
$R_i = \Sigma\lvert(F_o^2 - F_c^2)\rvert/F_o^2$	0.078
$R_p = \{\Sigma[y_i(\text{obs}) - y_i(\text{cal})/c]^2/\Sigma y_i(\text{obs})^2\}^{1/2}$	0.166
$R_{wp} = \{\Sigma w_i[y_i(o) - y_i(c)/c]^2/\Sigma w_i y_i(\text{obs})^2\}^{1/2}$	0.141
Preferred-orientation factor	0.31
Max shift/error	0.078

loss of the most volatile component, BaF_2, during heating, or that the reported composition for maximum deviation is slightly in error. A slight white coating, presumed to be BaF_2, was observed on the inside surface of the sealed quartz container which confined the specimen preparation boat. To check the composition the barium content was included as a variable after all other variables had reached minimum values. It stabilized at 0.66(4) with no significant change in other variables, indicative that the mixed composition had indeed lost some BaF_2. It is therefore presumed that the maximum angular deviation occurs at a slightly more Ba-rich composition.

Additional reflections which might be suggestive of superstructure and of cation ordering were not found. To determine how sensitive the powder diffraction patterns were to cation ordering, theoretical diffraction patterns were calculated for ordered models (*9*). The coordinates and thermal parameters derived in space group $P2/n$ were used in space group $P1$ with the Sr content confined to one site. The reflections forbidden in $P2/n$ calculated to an intensity of ~2 (scale of 100) in $P1$. It is unlikely that a reflection of that intensity could be seen in the Guinier photographs given the broadness of the reflections, and less likely that they would be visible in the diffractograms. Intensity differences between the two models were clearly smaller than preferred orientation effects. Hence it is impossible to determine on the basis of powder patterns if cation ordering occurs.

A plot of the observed and calculated intensity data is presented in Fig. 2. ESDs were calculated according to Scott (*10*) and are a factor of 5–7 times larger than those reported by the XRS82 system when this option is not used. Selected interatomic distances are presented in Table III. In the monoclinic phase some interatomic distances, i.e., F–F, Cl–Cl, are similar to those observed in BaFCl. It is interesting to note that, even considering the errors, the distances M–F or M–Cl, equivalent in the

TABLE II

FINAL POSITIONAL AND THERMAL PARAMETERS WITH THEIR ESDS FOR $Sr_{0.3}Ba_{0.7}FCl$

	x	y	z	U (Å^2)
Ba (=Sr)	0.25	0.25	0.204(1)	0.047(6)
Cl	0.25	0.25	0.649(4)	0.066(15)
F	0.75	0.25	−0.039(17)	0.066(41)

Note. Errors are calculated according to (*10*).

TABLE III

SELECTED BOND DISTANCES AND ESDS FOR $Sr_{0.3}Ba_{0.7}FCl$ AND RELATED STRUCTURES

	$Sr_{0.3}Ba_{0.7}FCl$		SrFCl (*8*)	BaFCl (*8*)
F–F	3.09(3)	3.11(3)	2.918(1)	3.1070(3)
F–Cl	3.11(9)	3.52(10)	3.229(3)	3.365(5)
F–Ba/Sr	2.45(6)	2.77(8)	2.494(1)	2.649(1)
Cl–Cl	3.71(2)	3.73(2)	3.531(3)	3.766(4)
Cl–Ba/Sr	3.18(3)	3.22(1)	3.072(4)	3.196(6)
	3.24(1) (2×)		3.112(1)	3.286(2)

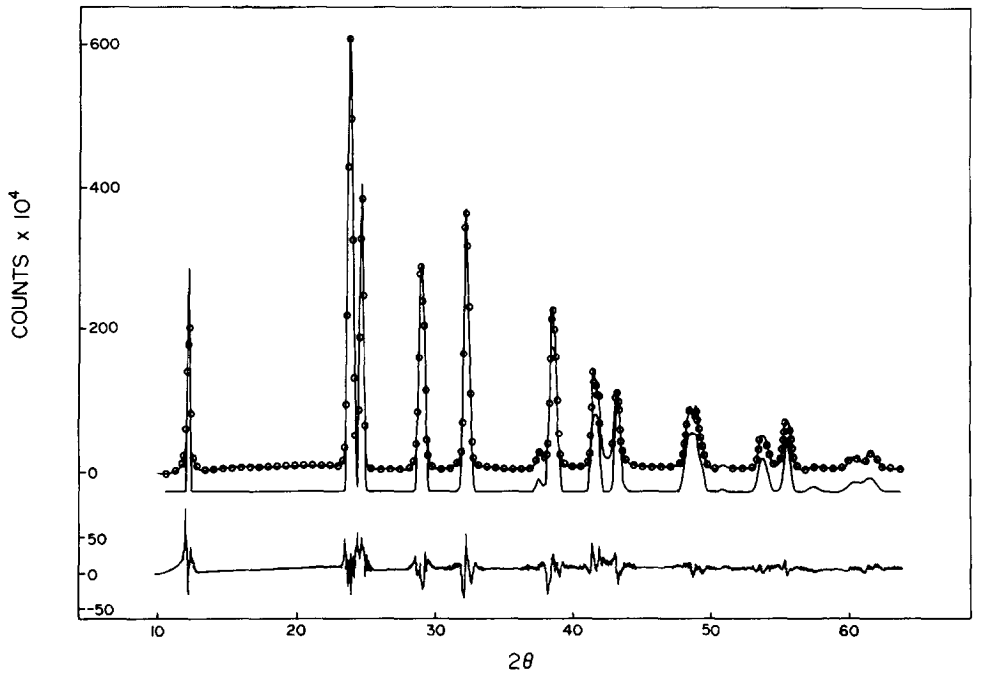

FIG. 2. Observed and calculated diffraction pattern for $Sr_{0.3}Ba_{0.7}FCl$ with a difference plot indicated at the base of the figure.

tetragonal cell, divide into two groups: one closer to *M*–F or *M*–Cl distances in SrFCl, and the other closer to the distances in BaFCl. The cations apparently strive to achieve a crystal environment similar to that which they had in BaFCl or SrFCl, suggestive of some degree of cation ordering. The intermediate region features characteristics of both parent phases; the monoclinic distortion in effect enables each cation to approximate its ideal environment. However, in a small cell ($Z = 2$) and for the composition $Sr_{0.3}Ba_{0.7}FCl$ constraints imposed by the crystal lattice prevent achievement of this ideal.

All $Sr_{0.3}Ba_{0.7}FCl$ specimens produced broad Guinier X-ray diffraction reflections regardless of whether they were air-quenched from the melt or cooled from 1000°C at the rate of 1°/min. Thus, the phase probably undergoes a transition from tetragonal to monoclinic symmetry at a temperature that is too low for the crystal growth needed for good X-ray diffraction to take place in the annealing times allowed.

The possibility that the crystals consisted of a diphasic tetragonal mixture was also considered. The crystals examined in the electron microscope were ~3 × 3 μm plates. Even though numerous diffraction patterns of single crystals were obtained and evaluated, it was difficult to characterize the small deviation from orthogonality accurately because of the angular sensitivity to crystal alignment. Based upon the (001) reciprocal lattice projection, the monoclinic angle determined from numerous zones was 89.7(5)°, within experimental error of orthogonality. However, a chemical indication of the crystalline character of the $Sr_{0.3}Ba_{0.7}FCl$ phase was found. Some monoclinic samples that were remelted and cooled exceedingly slowly were found to recrystallize to a mixture of two tetragonal

phases with lattice parameters very close to those of $Sr_{0.6}Ba_{0.4}FCl$ and $Sr_{0.1}Ba_{0.9}FCl$. The presence of these two phases suggests that the *equilibrium* solid solution region (*1*) is limited to the terminal SrFCl and BaFCl structure types. Lattice parameters reported previously (*1*) for $Sr_{0.6}Ba_{0.4}FCl$: a = 4.238(1), c = 7.064(8) Å (V = 126.9 Å^3); this work: a = 4.245(5), c = 7.033(8) Å (V = 126.73 Å^3). Parameters reported (*1*) for $Sr_{0.1}Ba_{0.9}FCl$: a = 4.370(4), c = 7.197(7) Å (V = 137.5 Å^3); this work: a = 4.347(6) and c = 7.119(5) Å (V = 134.5 Å^3). These observations suggest that the monoclinic $Sr_{0.3}Ba_{0.7}FCl$ is metastable. Under proper conditions it will recrystallize to other phases which have closely related structures. The metastable character of this compound would also explain the broad and somewhat diffuse character of the X-ray diffraction reflections.

The various R factors are consistent with those reported for X-ray Rietveld refinements, an indication of the correctness of the solution. The large ESDs are reflective both of the extensive overlapping of reflections and of their broadness. However, it is significant to note that even with less than optimum X-ray diffraction data, the Rietveld method allows a definitive structural solution to be achieved.

Acknowledgment

Support of the National Science Foundation, Division of Materials Research, Solid State Chemistry Program DMR-84-00739 is acknowledged gratefully.

References

1. S. A. Hodorowicz, E. K. Hodorowicz, and H. A. Eick, *J. Solid State Chem.* **50,** 180 (1983).
2. H. M. Rietveld, *J. Appl. Crystallogr.* **2,** 65 (1969).
3. J. Ladell, A. Zagofsky, and J. S. Pearlman, *J. Appl. Crystallogr.* **8,** 499 (1975).
4. Ch. Baerlocher and A. Hepp, "The X-Ray Rietveld System," Institut fuer Kristallogr. und Petrographie, ETH, Zurich (1982).
5. J. A. Ibers and W. C. Hamilton (Eds.), "International Tables for X-Ray Crystallography," Vol. 4, Kynoch Press, Birmingham (1974).
6. D. T. Cromer and J. B. Mann, *Acta Crystallogr. Sect. A* **24,** 321 (1968).
7. H. P. Klug and L. E. Alexander, "X-Ray Diffraction Procedures For Polycrystalline and Amorphous Materials," 2nd ed., Wiley, New York (1974).
8. M. Sauvage, *Acta Crystallogr. Sect. B* **30,** 2786 (1974).
9. D. K. Smith, M. C. Nichols, and M. E. Zolensky, "POWD 10: A FORTRAN IV Program for Calculating X-Ray Powder Diffraction Intensities, Version 10," Pennsylvania State University, University Park (1983).
10. H. G. Scott, *J. Appl. Crystallogr.* **16,** 159 (1983).